Divergent Performances of Vegetation Indices in Extracting Photosynthetic Phenology for Northern Deciduous Broadleaf Forests

Yajie Yang, Rui Chen, Gaofei Yin, *Senior Member, IEEE*, Cong Wang, Guoxiang Liu, Aleixandre Verger, Adrià Descals, Iolanda Filella, and Josep Peñuelas

***Abstract*— Accurate estimation of photosynthetic phenology is of great importance for understanding carbon cycles. Most vegetation indices (VIs) calculated from remotely sensed reflectances represent the canopy structure and have high uncertainty in detecting the photosynthetic phenology. We compared the start/end of the photosynthetically active season (SOS/EOS) extracted from the normalized difference vegetation index (NDVI), the enhanced vegetation index (EVI), the near-infrared reflectance of vegetation (NIRv), and the product of NIRv and solar incident radiation (NIRvP) over northern deciduous broadleaf forests (DBFs), and we used the metrics generated from solar-induced chlorophyll fluorescence (SIF), a proxy for photosynthesis, as reference. We found that the growing season extracted from the structural VIs was generally longer than the duration of photosynthetic activity retrieved from SIF: SOS derived from NDVI $<$ NIRvP $<$ EVI $\approx$ NIRv $\approx$ SIF and EOS from NDVI $>$ NIRv $\approx$ EVI $>$ NIRvP $\approx$ SIF. We investigated the mechanism underlying these phenological discrepancies using the paradigm of light-use efficiency (LUE). Our results show that the divergent performances of VIs were related to main factors limiting photosynthesis, which vary across different growth stages. The fraction of absorbed photosynthetically active radiation (FAPAR) absorbed by chlorophyll ($FAPAR_{chl}$) that is well characterized by both EVI and NIRv, was the dominant factor of spring photosynthetic phenology, whilst NIRvP that is a proxy of the total amount of photosynthetically active radiation absorbed by chlorophyll ($APAR_{chl}$) was the dominant factor in autumn when radiation determines photosynthetic phenology. As such, we suggest that these factors be accounted for when selecting VIs for the extraction of photosynthetic phenology, i.e., EVI and NIRv are more suitable for accurate retrieval of SOS, and NIRvP is more suitable for accurate retrieval of EOS.**

***Index Terms*— Deciduous broadleaf forest (DBF), light-use efficiency (LUE), photosynthetic phenology, vegetation indices (VIs).**

I. Introduction

THE annual growth and uptake of photosynthetic carbon by Northern deciduous broadleaf forests (DBFs) have strong seasonal cycles, which substantially influences the annual and interannual variation of atmospheric CO_2 concentrations [1]. Climatic warming has lengthened the growing season and increased the uptake of photosynthetic carbon by DBFs [2]. A better understanding of the photosynthetic phenology of DBFs is therefore necessary for more accurate predictions of future climate.

Satellite observations can provide spatiotemporally continuous observations over terrestrial surfaces. Most vegetation indices (VIs) extracted from satellite reflectances contain information about biomass greenness and have therefore been widely used to monitor large-scale terrestrial-surface phenology, which has greatly improved our understanding of seasonal productivity in recent decades [3]. Greenness VIs are generally reliable proxies for tracking the dynamics of gross primary productivity (GPP) but by nature represent vegetation structure, i.e., potential GPP, and cannot be directly converted to actual GPP, because plant photosynthesis is also constrained by environmental stress, as expressed by environmental scalars in models of light-use efficiency (LUE) [4]. As a result, divergent results have been reported between phenological metrics extracted using VIs and GPP [5], [6].

The performances of VIs in identifying the interannual variation in photosynthetic phenology remain highly uncertain [3]. For example, the commonly used normalized difference vegetation index (NDVI) scales well with the fraction of absorbed photosynthetically active radiation (FAPAR) but substantially overestimates the length of photosynthetic phenology derived from tower-based measurements of GPP [7] indicating a systematic bias in seasonality between plant structure and function [3]. In comparison, the enhanced vegetation index (EVI) is more sensitive to FAPAR absorbed by chlorophyll ($FAPAR_{chl}$) [8], so EVI outperforms NDVI in extracting

Manuscript received April 6, 2022; revised May 27, 2022; accepted June 7, 2022. Date of publication June 13, 2022; date of current version June 22, 2022. This work was supported in part by the National Natural Science Foundation of China under Grant 41971282 and in part by the Sichuan Science and Technology Program under Grant 2021JDJQ0007 and Grant 2020JDTD0003. The work of Aleixandre Verger, Adrià Descals, Iolanda Filella, and Josep Peñuelas was supported in part by the Spanish Government under Grant PID2019-110521GB-I00, in part by the Fundación Ramón Areces under Grant CIVP20A6621, and in part by the Catalan Government under Grant SGR2017-1005. *(Corresponding author: Gaofei Yin.)*

Yajie Yang, Rui Chen, and Gaofei Yin are with the Faculty of Geosciences and Environmental Engineering, Southwest Jiaotong University, Chengdu 610031, China (e-mail: yingf@swjtu.edu.cn).

Cong Wang is with the Key Laboratory for Geographical Process Analysis and Simulation of Hubei Province, School of Urban and Environmental Sciences, Central China Normal University, Wuhan 430079, China.

Guoxiang Liu is with the Faculty of Geosciences and Environmental Engineering, Southwest Jiaotong University, Chengdu 610031, China, and also with the State-Province Joint Engineering Laboratory of Spatial Information Technology for High-Speed Railway Safety, Chengdu 610031, China.

Aleixandre Verger is with CIDE, CSIC-UV-GVA, 46113 València, Spain, also with CREAF, Cerdanyola del Vallès, Barcelona, 08193 Catalonia, Spain, and also with CSIC, Global Ecology Unit CREAF-CSIC-UAB, Barcelona, 08193 Catalonia, Spain.

Adrià Descals, Iolanda Filella, and Josep Peñuelas are with CREAF, Cerdanyola del Vallès, Barcelona, 08193 Catalonia, Spain, and also with CSIC, Global Ecology Unit CREAF-CSIC-UAB, Barcelona, 08193 Catalonia, Spain.

Digital Object Identifier 10.1109/LGRS.2022.3182405

photosynthetic phenology because chlorophyll is a robust proxy for foliar photosynthetic capacity [9]. Other studies, however, found that the length of the photosynthetically active season derived from EVI also overestimated the actual active season in DBFs by two week [10], [11]. The near-infrared reflectance of vegetation (NIRv) [12], another popular VI in the phenological community, performed comparably with EVI in extracting photosynthetic phenology [3]. NIRvP, expressed as the product of NIRv and solar incident radiation, is an improved version of NIRv and is a robust structural proxy of GPP [13]. Its performance in extracting photosynthetic phenology, however, remains unclear.

Solar-induced chlorophyll fluorescence (SIF) is a small part of the 650–680 nm electromagnetic signal re-emitted by chlorophyll after absorbing sunlight during photosynthesis and can be directly detected by satellite sensors [14]. In contrast to information about green biomass identified by structural VIs, SIF is mechanistically linked with photosynthesis and therefore can respond quickly to nearly all factors regulating photosynthetic activity [14]. Many recent studies have demonstrated the rationality of using SIF in extracting photosynthetic phenology, and the results can be used as reference values to validate the performance of VIs [7], [15].

In summary, commonly used VIs were designed to represent plant structure and greenness rather than physiology, so the derived phenology characterizes the seasonal variation in potential GPP, which systematically overestimates the actual GPP. Very few studies have been devoted to comparing the photosynthetic phenology extracted from structural VIs, especially from the newly developed VIs. We compared the start and end of the photosynthetically active season in northern DBFs using NDVI, EVI, NIRv, and NIRvP, using the metrics generated from SIF as baseline. We hypothesize that the terrestrial surface phenology derived from structural VIs has a systematic bias compared with photosynthetic phenology in DBFs, and we investigated the underlying mechanism of this divergence.

II. Materials and Methods

A. Study Area

This study focused on the northern (≥30°N) DBFs, which are generally in regions with moist, warm summers and frosty winters, in three main areas: 1) Eastern North America; 2) Western and Central Europe; and 3) Eastern Asia. The leaves unfold in spring as temperatures increase, senesce, and then fall in autumn with the shortening of the photoperiod and the declining of the temperature [7].

B. Datasets and Indices

MODIS: The VIs were calculated using surface reflectance from the MCD43A4 Version 6 product, which is adjusted to nadir from multiangular, cloud-free, atmospherically corrected measurements using a bidirectional reflectance distribution function (BRDF) for the solar angle at local noontime [16]. MCD43A4 is produced daily based on 16 d retrieval period of Terra and Aqua MODIS data at a resolution of 500 m. Low-quality (magnitude BRDF inversions) and snow-contaminated observations were removed before analysis based on the quality flag.

TABLE I
Definition of the VIs Tested in This Study

Vegetation index	Reference
$NDVI = \frac{NIR - R}{NIR + R}$	[20]
$EVI = 2.5 \cdot \frac{NIR - R}{NIR + 6R - 7.5B - 1}$	[21]
$NIRv = \frac{NIR - R}{NIR + R} \cdot NIR$	[12]
$NIRvP = \frac{NIR - R}{NIR + R} \cdot NIR \cdot PAR$	[13]

R, *B* and *NIR* are the MODIS reflectances at the red, blue and near-infrared bands, respectively. Photosynthetically active radiation (PAR) is represented by ERA5-Land shortwave radiation.

GOSIF: GOSIF, with a spatial resolution of 0.05 × 0.05° and a revisit time of 8 d, was used as a reference to extract photosynthetic phenology. It was produced by a machine-learning method using discrete OCO-2 SIF, MCD43C4 reflectance, and MERRA-2 meteorological data as inputs. The strong correlation between GOSIF and GPP has been verified at 91 FLUXNET sites across the world ($R^2 = 0.73$, $p < 0.001$) [17].

ERA5-Land: The solar incident radiation (also known as shortwave radiation) provided by ERA5-Land was used to represent the photosynthetically active radiation (PAR). ERA5-Land is the fifth generation of climate reanalysis dataset produced by the European Centre for Medium-Range Weather Forecasts (ECMWF), with a spatial resolution of 0.1° and a temporal resolution of 1 h [18]. The daily maximum was selected to represent daily value.

CCI land cover: The land-cover products released by the Land Cover Climate Change Initiative (CCI) of the European Space Agency provides global land-cover maps at a spatial resolution of 300 m on an annual basis [19]. CCI divides the terrestrial surface into 22 classes, which have been defined using the United Nations Food and Agriculture Organization's Land Cover Classification System. We aggregated the land-cover products into 0.05 × 0.05° through the nearest neighbor method and delineated DBF without land type change from 2001 to 2020.

Selected indices: We selected four commonly used VIs for comparing their performances in extracting photosynthetic phenology. They were computed using MODIS reflectances and ERA5-Land data. The formulations of the VIs are presented in Table I.

C. Extraction of Phenology

Our study period was from 2001 to 2020, representing maximum temporal overlaps of all datasets used. We first aggregated the VIs derived from MODIS and ERA5-Land data into a resolution of 0.05 × 0.05° and 8 d through an averaging method. The VIs values for different years were averaged every 8 d to obtain their annual climatologies. We then used three methods, Savitzky–Golay (SG), asymmetric Gaussian (AG), and double logistic (DL), to smooth the climatological data. SG filtering is a quadratic fitting method based on the local characteristics of a curve. We set the half-window to

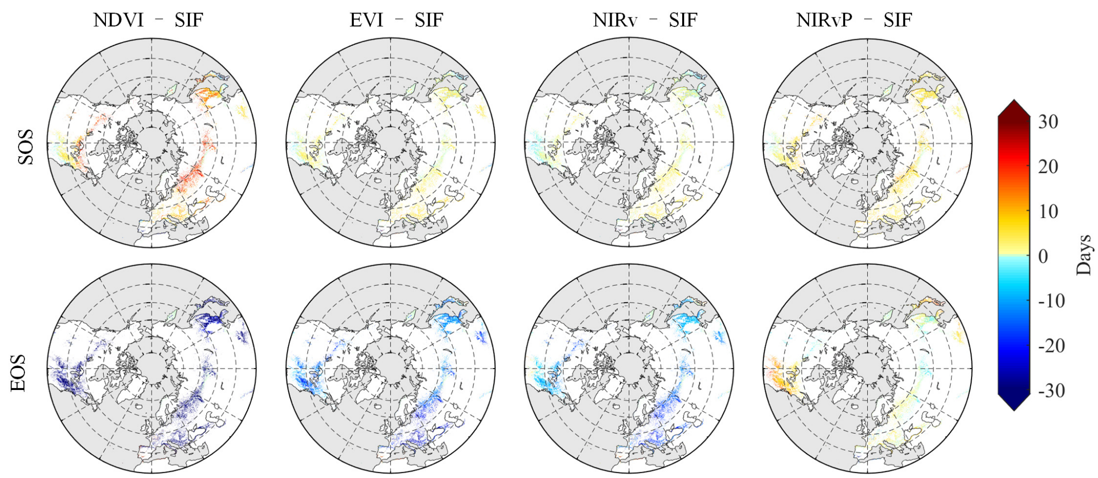

Fig. 1. Spatial distribution of temporal mismatches between phenological metrics derived from the VIs and those from sun-induced fluorescence. The NDVI, EVI, NIRv, and NIRv multiplied by incoming sunlight (NIRvP) were used to estimate the start and end of the growing season (SOS and EOS).

32 d to ensure a high degree of smoothness. Both the AG and DL methods perform least-square fitting to the data with corresponding functions and use the fitted curve to replace the original time series. Detailed information about the three methods are provided by [22]. Smoothing was implemented using TIMESAT software [22].

The start of the photosynthetically active season (SOS) and the end of the photosynthetically active season (EOS) were then extracted using the dynamic-threshold method [22]. Specifically, we adopted the threshold of 50% of the annual amplitude. SOS occurs when the left side of the reconstructed time-series curve before the annual maximum has reached half the amplitude, counted from the base level. EOS is defined similarly, but for the right side of the curve after the annual maximum. The SOS and EOS values extracted from the reconstructed climatologies of VIs and SIFs with the three smoothing methods, i.e., SG, AG, and DL, were averaged at pixel scale to obtain robust estimates of phenology metrics.

D. Model of LUE

We interpreted the divergent performances of the VIs using the LUE paradigm. LUE assumes that plant photosynthesis is jointly controlled by changes in PAR, $FAPAR_{chl}$, and LUE [4], i.e., $GPP = PAR \times FAPAR_{chl} \times LUE = APAR_{chl} \times LUE$, where $APAR_{chl}$ is the amount of PAR absorbed by chlorophyll, i.e., $PAR \times FAPAR_{chl}$.

At the seasonal scale, PAR is directly associated with the solar zenith angle and cloud cover, $FAPAR_{chl}$ depends on canopy structure and amount of foliar chlorophyll and LUE denotes LUE under a specific environment at the canopy scale and may vary with factors such as the phenological period (LUE shows diurnal, seasonal, and long term variations), physiological conditions (e.g., nutrient levels) and climatic conditions (temperature and water stress) [23].

III. RESULTS

The spatial distribution of the temporal mismatches among the phenological metrics of northern DBFs based on the VIs is shown in Fig. 1. SOS generally had smaller mismatches across all indices compared with EOS, with histograms centered near zero (Fig. 2). NDVI- and NIRvP-derived estimates of SOS were an average of 11 and 6 d earlier than the SIF-derived estimates, respectively. EVI- and NIRv-derived SOSs were very similar and were only 2 d earlier than the reference values. The differences in EOSs across all indices were very distinct, with histograms centered far from zero. NIRvP was the only exception [Fig. 2(b)]. NDVI-, EVI-, and NIRv-derived estimates of EOS averaged 42, 14, and 13 d later than the SIF-derived estimates, whereas NIRvP performed very well in extracting EOSs, with a bias of only −2 d indicating earlier EOS for NIRvP than SIF.

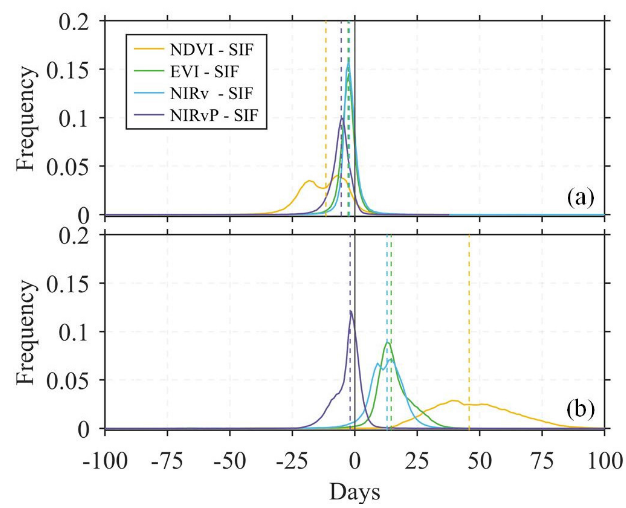

Fig. 2. Frequency distribution of temporal mismatches between phenological metrics derived from the VIs and those from sun-induced fluorescence. The NDVI, EVI, NIRv, and NIRv multiplied by incoming sunlight (NIRvP) were used to estimate (a) start and (b) end of the growing season (SOS and EOS). The vertical dotted lines represent the average temporal differences in phenological metrics from different proxies.

We further compared the timing of the phenological metrics by latitude (Fig. 3). We considered the range of latitudes 30°N–60°N where most of the world's DBFs locate (Fig. 1). SOSs from all indicators had good consistency at mid-low latitudes (30°N–40°N) [Fig. 3(a)]. SOS from each index occurred later as latitude increased. Averaged SOSs derived from SIF,

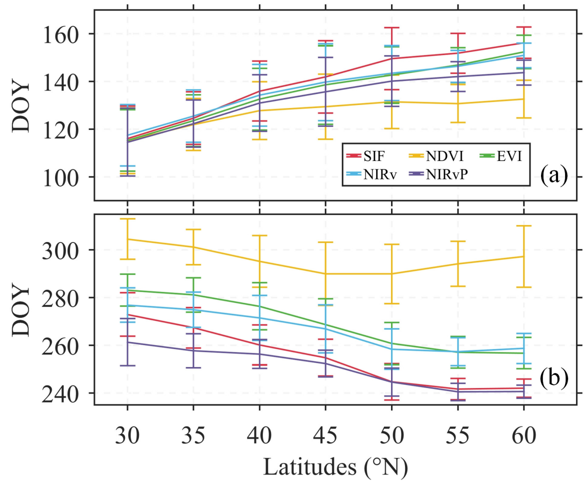

Fig. 3. Latitudinal distribution of averaged (a) start and (b) end of the growing season derived from sun-induced fluorescence, NDVI, EVI, NIRv, and NIRv multiplied by incoming sunlight (NIRvP). Error bars indicate regional standard deviations. DOY: day of year.

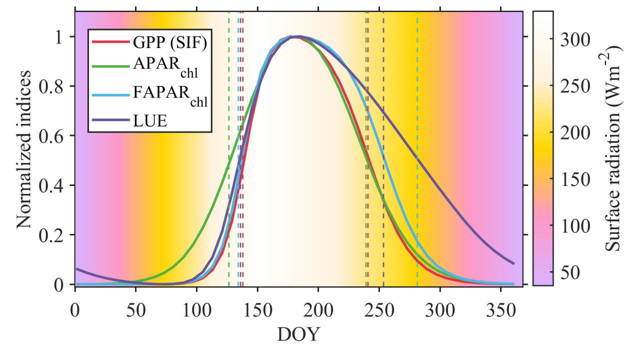

Fig. 4. Seasonality of GPP, absorbed photosynthetic active radiation absorbed by chlorophyll ($APAR_{chl}$), $FAPAR_{chl}$, and LUE. All indicators were linearly normalized to [0, 1] for visualization. The background colors represent the change of surface radiation. DOY: day of year.

EVI, NIRv, NIRvP, and NDVI at high latitudes (50°N–60°N) were about 40, 36, 34, 29, and 17 d later than those at mid-low latitudes, respectively. The divergence of VI-derived SOS, compared with the SIF-derived reference, correspondingly increased with latitude. NDVI- and NIRvP-derived SOSs at high latitudes had larger deviations from SIF-derived SOS, and their estimated SOSs were 24 and 13 d earlier than that estimated by SIF, respectively. EVI-derived SOS nearly coincided with NIRv-derived SOS and occurred only about 4 d earlier than SIF-derived SOS at high latitudes. In contrast, EOS in autumn from all indicators advanced as the latitude increased [Fig. 3(b)]. NIRvP-derived EOS approximated the SIF-derived EOS very well, especially at high latitudes, with a bias of only 1 d. EVI- and NIRv-derived EOSs were consistent, about 15 d later than SIF-derived EOS at high latitudes. As for NDVI-derived EOS, an averaged 41 d lag across all the latitude bands, compared with SIF-derived one, was observed. However, the latitudinal gradient of EOS was not detected from NDVI.

IV. Discussion

VIs extracted from reflectances have been widely used to estimate photosynthetic phenology. We found deviations in the photosynthetic phenology extracted by different VIs over the northern DBFs (Figs. 1–3). Interpretation of physical meanings of VIs and their divergent performances in tracking photosynthetic phenology can be explained using the LUE paradigm. NDVI is widely used as a robust proxy of FAPAR [24], but not all PAR absorbed by a canopy can be used for photosynthesis. PAR at the canopy scale will be absorbed by both chlorophyll and nonphotosynthetic vegetation (e.g., stems, branches, and senescent leaves) [8], [25]. Only the light absorbed by chlorophyll forces photosynthesis. EVI, the proxy of $FAPAR_{chl}$, was therefore preferred for estimating GPP in recent studies [8], [25]. EVI has been strongly correlated with $FAPAR_{chl}$ ($R^2 = 0.97$) [25]. EVI and NIRv in our study provided similar results in monitoring photosynthetic phenology (Figs. 1–3), consistent with [3] and [26]. NIRv can therefore also act as a proxy of $FAPAR_{chl}$. NIRvP, the product of NIRv, and PAR introduces the limitation of external radiation to NIRv, which can be regarded as a powerful proxy of $APAR_{chl}$, i.e., $FAPAR_{chl} \times PAR = APAR_{chl}$. Another study also found that NIRvP was a robust proxy for far-red SIF across a wide range of spatial and temporal scales [13]. We depicted the averaged seasonality of GPP (represented by SIF), $FAPAR_{chl}$ (by EVI), $APAR_{chl}$ (by EVI $\times$ PAR), and LUE [by SIF/(EVI $\times$ PAR)] over the northern DBF. The curves for both $FAPAR_{chl}$ and LUE in spring were similar to the curve for GPP, whilst the curve for $APAR_{chl}$ was very different. In contrast, the curves for $APAR_{chl}$ and GPP in autumn generally overlapped with each other, whilst deviations were larger between $FAPAR_{chl}$ and for LUE, especially. Closer inspection showed that autumn phenology is more radiation limited than spring phenology. These results highlighted that VIs performed differently in tracking GPP across different growth stages.

Vegetation needs time to resume primary productivity in spring after leaf-budding by absorbing carbon [7]. The timing of the lag of carbon assimilation behind leaf emergence in spring was thus consistent with the trends of lag of spring SIF behind VI-based spring phenology [Fig. 2(a)]. Vegetation photosynthesis increased with $FAPAR_{chl}$ when available incoming solar radiation was sufficient and temperatures were favorable (Fig. 4), so the canopy chlorophyll content may be the main factor affecting the phenology, as also reported by [9] that canopy chlorophyll content was strongly correlated with photosynthetic capacity. Photosynthesis always shuts down in autumn before leaf-drop [27], because plant photosynthesis in autumn is limited by the availability of light with the rapid decline of solar radiation [6]. This shutdown is consistent with our finding that plant photosynthesis decreased as $APAR_{chl}$ decreased (Fig. 4). Insufficient radiation inhibits the physiology of vegetation, i.e., the vegetation cannot use enough light for photosynthesis even though chlorophyll still remains, accounting for the deviation of $FAPAR_{chl}$ from GPP.

Different VIs generally contain different types of information about photosynthesis, so we suggest that VIs should be dedicatedly selected for improving the extraction of photosynthetic phenology. For example, chlorophyll content in spring dominates the rate of carbon sequestration, so VIs containing information about chlorophyll, e.g., EVI and NIRv, can reliably estimate SOS. Low radiation level in autumn and at high latitudes limits canopy photosynthesis. VIs containing information about radiation, e.g., NIRvP, may therefore be the best choice for extracting EOS. The combination of multiple VIs will help to improve our understanding of terrestrial ecosystems and the carbon cycle.

We used the metrics generated from SIF as baseline for photosynthetic phenology assuming SIF as a proxy of GPP. Recent studies demonstrated that phenological metrics derived from SIF highly agree with those from GPP and SIF closely track the seasonal changes in plant photosynthesis [7], [15]. Environmental stress factors (e.g., drought stress and heatwaves) may break down the linearity between SIF and GPP [28], but these cases are beyond the scope of this letter.

V. Conclusion

We compared the performances of four commonly used VIs, NDVI, EVI, NIRv, and NIRvP, in the extraction of the start and end of the photosynthetically active season over northern DBF regions, using metrics generated from SIF as baseline. The LUE paradigm was used to identify the mechanism of the discrepancy in the extracted phenological metrics. In spring, EVI/NIRv-extracted SOS nearly coincided with the initiation of carbon assimilation, but SOS extracted from NIRvP/NDVI had larger deviations compared with that extracted from SIF (6 and 11 d earlier for NDVI and NIRvP, respectively). In autumn, NDVI-derived EOS lagged greatly (42 d) and EVI/NIRv-derived EOS lagged slightly (13/14 d) behind SIF-derived EOS. In comparison, NIRvP approximated SIF very well, with the bias decreasing to only 2 d. The divergent performances of the VIs in extracting photosynthetic phenology indicated that the main factors limiting photosynthesis differed among the stages of growth. VIs associated with $FAPAR_{chl}$, e.g., EVI and NIRv, and VIs associated with $APAR_{chl}$, e.g., NIRvP, are respectively recommended for extracting the timing of the start and end of the photosynthetically active season. Our study will contribute to a better understanding of the divergence in the phenological shifts in greenness and photosynthesis, which is crucial for accurate modeling of carbon cycling and atmospheric CO_2 concentration.

Acknowledgment

This study contributes to the CSIC Thematic Interdisciplinary Platform PTI TELEDETECT (CSIC PTI-TELEDETECT).

References

[1] C. D. Keeling, J. F. S. Chin, and T. P. Whorf, “Increased activity of northern vegetation inferred from atmospheric CO_2 measurements,” *Nature*, vol. 382, no. 6587, pp. 146–149, Jul. 1996.

[2] T. F. Keenan *et al.*, “Net carbon uptake has increased through warming-induced changes in temperate forest phenology,” *Nature Climate Change*, vol. 4, no. 7, pp. 598–604, 2014.

[3] G. Yin, A. Verger, I. Filella, A. Descals, and J. Peñuelas, “Divergent estimates of forest photosynthetic phenology using structural and physiological vegetation indices,” *Geophys. Res. Lett.*, vol. 47, no. 18, Sep. 2020, Art. no. e2020GL089167.

[4] J. L. Monteith, “Solar radiation and productivity in tropical ecosystems,” *J. Appl. Ecol.*, vol. 9, no. 3, p. 747, Dec. 1972.

[5] Q. Xie *et al.*, “Land surface phenology retrievals for arid and semi-arid ecosystems,” *ISPRS J. Photogramm. Remote Sens.*, vol. 185, pp. 129–145, Mar. 2022.

[6] Y. Zhang, R. Commane, S. Zhou, A. P. Williams, and P. Gentine, “Light limitation regulates the response of autumn terrestrial carbon uptake to warming,” *Nature Climate Change*, vol. 10, no. 8, pp. 739–743, Aug. 2020.

[7] S.-J. Jeong *et al.*, “Application of satellite solar-induced chlorophyll fluorescence to understanding large-scale variations in vegetation phenology and function over northern high latitude forests,” *Remote Sens. Environ.*, vol. 190, pp. 178–187, Mar. 2017.

[8] X. Xiao, “Light absorption by leaf chlorophyll and maximum light use efficiency,” *IEEE Trans. Geosci. Remote Sens.*, vol. 44, no. 7, pp. 1933–1935, Jul. 2006.

[9] H. Croft, J. M. Chen, X. Luo, P. Bartlett, B. Chen, and R. M. Staebler, “Leaf chlorophyll content as a proxy for leaf photosynthetic capacity,” *Global Change Biol.*, vol. 23, no. 9, pp. 3513–3524, Sep. 2017.

[10] P. D’Odorico *et al.*, “The match and mismatch between photosynthesis and land surface phenology of deciduous forests,” *Agricult. Forest Meteorol.*, vols. 214–215, pp. 25–38, Dec. 2015.

[11] M. Shen, Y. Tang, A. R. Desai, C. Gough, and J. Chen, “Can EVI-derived land-surface phenology be used as a surrogate for phenology of canopy photosynthesis?” *Int. J. Remote Sens.*, vol. 35, no. 3, pp. 1162–1174, Feb. 2014.

[12] G. Badgley, C. B. Field, and J. A. Berry, “Canopy near-infrared reflectance and terrestrial photosynthesis,” *Sci. Adv.*, vol. 3, no. 3, Mar. 2017, Art. no. e1602244.

[13] B. Dechant *et al.*, “NIRVP: A robust structural proxy for sun-induced chlorophyll fluorescence and photosynthesis across scales,” *Remote Sens. Environ.*, vol. 268, Jan. 2022, Art. no. 112763.

[14] A. Porcar-Castell *et al.*, “Linking chlorophyll a fluorescence to photosynthesis for remote sensing applications: Mechanisms and challenges,” *J. Experim. Botany*, vol. 65, pp. 4065–4095, Aug. 2014.

[15] Z. Pierrat *et al.*, “Diurnal and seasonal dynamics of solar-induced chlorophyll fluorescence, vegetation indices, and gross primary productivity in the boreal forest,” *J. Geophys. Res., Biogeosci.*, vol. 127, no. 2, Feb. 2022, Art. no. e2021JG006588.

[16] C. B. Schaaf *et al.*, “First operational BRDF, albedo nadir reflectance products from MODIS,” *Remote Sens. Environ.*, vol. 83, nos. 1–2, pp. 135–148, 2002.

[17] X. Li and J. Xiao, “A global, 0.05-degree product of solar-induced chlorophyll fluorescence derived from OCO-2, MODIS, and reanalysis data,” *Remote Sens.*, vol. 11, no. 5, p. 517, Mar. 2019.

[18] J. Muñoz-Sabater *et al.*, “ERA5-land: A state-of-the-art global reanalysis dataset for land applications,” *Earth Syst. Sci. Data*, vol. 13, no. 9, pp. 4349–4383, Sep. 2021.

[19] S. Bontemps *et al.*, “Multi-year global land cover mapping at 300 m and characterization for climate modelling: Achievements of the land cover component of the ESA climate change initiative,” *Int. Arch. Photogramm. Remote Sens. Spatial Inf. Sci.*, vol. XL-7/W3, pp. 323–328, May 2015.

[20] J. W. Rouse, R. H. Haas, J. A. Schell, and D. W. Deering, “Monitoring vegetation systems in the great plains with ERTS,” in *Proc. 3rd ERTS Symp., NASA (SP)*, vol. 1, 1974, pp. 309–317.

[21] H. Q. Liu and A. Huete, “A feedback based modification of the NDVI to minimize canopy background and atmospheric noise,” *IEEE Trans. Geosci. Remote Sens.*, vol. 33, no. 2, pp. 457–465, Mar. 1995.

[22] P. Jönsson and L. Eklundh, “TIMESAT—A program for analyzing time-series of satellite sensor data,” *Comput. Geosci.*, vol. 30, no. 8, pp. 833–845, Oct. 2004.

[23] M. F. Garbulsky, I. Filella, A. Verger, and J. Peñuelas, “Photosynthetic light use efficiency from satellite sensors: From global to Mediterranean vegetation,” *Environ. Experim. Botany*, vol. 103, pp. 3–11, Jul. 2014.

[24] R. B. Myneni and D. L. Williams, “On the relationship between FAPAR and NDVI,” *Remote Sens. Environ.*, vol. 49, no. 3, pp. 200–211, Sep. 1994.

[25] Y. Zhang *et al.*, “Spatio-temporal convergence of maximum daily light-use efficiency based on radiation absorption by canopy chlorophyll,” *Geophys. Res. Lett.*, vol. 45, no. 8, pp. 3508–3519, Apr. 2018.

[26] C. Wang *et al.*, “Phenology dynamics of dryland ecosystems along the north Australian tropical transect revealed by satellite solar-induced chlorophyll fluorescence,” *Geophys. Res. Lett.*, vol. 46, no. 10, pp. 5294–5302, May 2019.

[27] F. Daumard *et al.*, “A field platform for continuous measurement of canopy fluorescence,” *IEEE Trans. Geosci. Remote Sens.*, vol. 48, no. 9, pp. 3358–3368, Sep. 2010.

[28] D. Martini *et al.*, “Heatwave breaks down the linearity between sun-induced fluorescence and gross primary production,” *New Phytolog.*, vol. 233, no. 6, pp. 2415–2428, Mar. 2022.